Rapid decay of nonlinear whistler waves in two dimensions: Full particle simulation

Takayuki Umeda, Shinji Saito, and Yasuhiro Nariyuki

Citation: Physics of Plasmas **24**, 054503 (2017); doi: 10.1063/1.4982609
View online: http://dx.doi.org/10.1063/1.4982609
View Table of Contents: http://aip.scitation.org/toc/php/24/5
Published by the American Institute of Physics

Rapid decay of nonlinear whistler waves in two dimensions: Full particle simulation

Takayuki Umeda,[1,a)] Shinji Saito,[1,2] and Yasuhiro Nariyuki[3]
[1]*Institute for Space-Earth Environmental Research, Nagoya University, Nagoya 464-8601, Japan*
[2]*Graduate School of Science, Nagoya University, Nagoya 464-8602, Japan*
[3]*Faculty of Human Development, University of Toyama, Toyama 930-8555, Japan*

(Received 13 January 2017; accepted 13 April 2017; published online 26 April 2017)

The decay of a nonlinear, short-wavelength, and monochromatic electromagnetic whistler wave is investigated by utilizing a two-dimensional (2D) fully relativistic electromagnetic particle-in-cell code. The simulation is performed under a low-beta condition in which the plasma pressure is much lower than the magnetic pressure. It has been shown that the nonlinear (large-amplitude) parent whistler wave decays through the parametric instability in a one-dimensional (1D) system. The present study shows that there is another channel for the decay of the parent whistler wave in 2D, which is much faster than in the timescale of the parametric decay in 1D. The parent whistler wave decays into two sideband daughter whistlers propagating obliquely with respect to the ambient magnetic field with a frequency close to the parent wave and two quasi-perpendicular electromagnetic modes with a frequency close to zero via a 2D decay instability. The two sideband daughter oblique whistlers also enhance a nonlinear longitudinal electrostatic wave via a three-wave interaction as a secondary process. *Published by AIP Publishing.*
[http://dx.doi.org/10.1063/1.4982609]

It has been known that large-amplitude and monochromatic plasma waves are often unstable nonlinearly. One of the well-known instabilities for large-amplitude parent waves is the parametric instability, in which a forward-propagating parent wave (P_0) decays into a backward-propagating daughter (D_1) wave and a forward-propagating sound wave (S_1), i.e., $P_0 \rightarrow D_1 + S_1$, which is also referred as the parametric decay. There is a number of studies in a one-dimensional (1D) spatial system for parametric instabilities of various finite-amplitude parent plasma waves, such as circularly polarized Alfvén waves,[1,2] (right-handed-polarized) high-frequency whistler waves,[3,4] high-frequency (light mode) radio waves,[5] and Langmuir waves.[6,7]

Our previous 1D particle-in-cell (PIC) simulation study has (re)confirmed that the parametric decay of a finite-amplitude ($\delta B^2 \sim 0.1 B_0^2$) and monochromatic whistler wave with a frequency close to the electron cyclotron frequency ω_{ce} takes place at a timescale of several hundreds of the electron cyclotron period. In the present study, we extend our previous 1D simulation study to a 2D one for examining a nonlinear development of an electron-scale, finite-amplitude, and monochromatic electromagnetic whistler wave with a frequency close to the electron cyclotron frequency in a self-consistent manner. We show that the decay of the parent whistler wave in 2D takes place much faster than in 1D. The present 2D decay process is different from the one seen in the previous 2D simulation of ion-scale whistler waves.[8]

A higher-order interpolation[9] is combined to the charge conservation scheme[10] in a standard 2D fully relativistic electromagnetic PIC code to reduce numerical noises. An initial condition is identical to our previous 1D simulation study.[4] A one-dimensional, single, sinusoidal, and right-hand-polarized electromagnetic plasma wave mode is imposed in a 2D doubly periodic system as a function of x only

$$B_y[x] = \delta B \sin[k_{x0}x - \omega_0 t + \phi], \tag{1}$$

$$B_z[x] = \delta B \cos[k_{x0}x - \omega_0 t + \phi], \tag{2}$$

$$E_y[x] = \frac{\omega_0}{k_{x0}} \delta B \cos[k_{x0}x - \omega_0 t + \phi], \tag{3}$$

$$E_z[x] = -\frac{\omega_0}{k_{x0}} \delta B \sin[k_{x0}x - \omega_0 t + \phi], \tag{4}$$

with $t = 0$ and ϕ being a random phase ($\phi = 0$ is chosen in the present study). An ambient magnetic field with an amplitude of B_0 is imposed in the x direction. One can easily find that the applied electromagnetic fluctuations satisfy one of Maxwell's equations

$$\frac{\partial \boldsymbol{B}}{\partial t} = -\nabla \times \boldsymbol{E}. \tag{5}$$

To satisfy another Maxwell's equation

$$\frac{1}{c^2}\frac{\partial \boldsymbol{E}}{\partial t} = \nabla \times \boldsymbol{B} - \mu_0 \boldsymbol{J}, \tag{6}$$

we need an electric current.

In the present study, we assume that the electric current is imposed by electrons only, i.e., $\boldsymbol{J} \sim \boldsymbol{J}_e = -eN_e\boldsymbol{U}_e$. At the initial state, we also assume that ions and electrons are distributed uniformly in the 1D system with the density $N_e = N_i = N_0$. Both ions and electrons have an isotropic shifted Maxwellian momentum distribution

a)Email: taka.umeda@nagoya-u.jp

$$f_{e(i)}[\boldsymbol{p}] = \frac{N_0}{\left(\sqrt{2\pi}V_{te(i)}\right)^3}\exp\left[-\frac{|\boldsymbol{p}-m_{e(i)}\boldsymbol{U}_{e(i)}|^2}{2m_{e(i)}^2V_{te(i)}^2}\right]. \quad (7)$$

Then, the electron bulk velocity (or electron velocity fields) $\boldsymbol{U}_e$ is obtained as

$$U_{y,e}[x] = \frac{k_{x0}^2c^2-\omega_0^2}{\omega_{pe}^2}\frac{\omega_{ce}}{k_{x0}}\frac{\delta B}{B_0}\sin[k_{x0}x-\omega_0t+\phi], \quad (8)$$

$$U_{z,e}[x] = \frac{k_{x0}^2c^2-\omega_0^2}{\omega_{pe}^2}\frac{\omega_{ce}}{k_{x0}}\frac{\delta B}{B_0}\cos[k_{x0}x-\omega_0t+\phi], \quad (9)$$

where $\omega_{pe}=\sqrt{e^2N_0/\epsilon_0m_e}$ and $\omega_{ce}=-eB_0/m_e$ are the electron plasma and cyclotron frequencies, respectively. Note that $\omega_{ce}<0$ for right-hand polarized waves and that $U_{x,e}=0$. The bulk velocity of ions is set to $\boldsymbol{U}_i=0$ as we assumed an electron current.

We use an empirical model of the linear dispersion equation for electromagnetic whistler waves based on the cold plasma equations[11] to obtain the frequency of the imposed wave mode

$$\omega_0 = |\omega_{ce}|\frac{|\boldsymbol{k}_0|k_{x0}c^2}{\omega_{pe}^2+\left(1+\sqrt{\beta_e}\right)|\boldsymbol{k}_0|^2c^2}, \quad (10)$$

where $\beta_{e(i)}=2\omega_{pe(i)}^2V_{te(i)}^2/\omega_{ce(i)}^2c^2=2\mu_0N_{e(i)}T_{e(i)}/B_0^2$ is the ratio of the electron (ion) plasma thermal pressure to the magnetic pressure (so-called plasma beta) with $V_{te(i)}=\sqrt{T_{e(i)}/m_{e(i)}}$ being the electron (ion) thermal velocity. It is noted that the above dispersion relation is an exact solution in the fluid limit.

The real mass ratio $m_i/m_e=1836$ is used, and the equal temperature $T_i=T_e=T_0$ is assumed. The grid spacing, the time step, and the speed of light are set as $\Delta x=\lambda_{De}=V_{te}/\omega_{pe}$, $\omega_{pe}\Delta t=0.005$, and $c=100V_{te}$, respectively. The number of grid points is $N_x=5120$ and $N_y=1280$. Thus, the system length is $L_x\times L_y=5120\lambda_{De}\times1280\lambda_{De}=51.2d_e\times12.8d_e$, where $d_e=c/\omega_{pe}$ is the electron inertial length. The number of particles per cell is 256 for each of the ion and electron components. The ratio of the electron plasma frequency to the electron cyclotron frequency is set as $\omega_{ce}/\omega_{pe}=-0.2236$, which correspond to the initial electron beta of $\beta_{e0}=0.004$.

The wavenumber of the parent right-hand-polarized electromagnetic plasma wave is $k_{x0}d_e=3.927$ (which corresponds to Mode 32 in the x direction) and $k_{y0}=0$. The frequency of the parent wave is given from Eq. (10) as $\omega_0=0.8865|\omega_{ce}|(=0.1982\omega_{pe})$. Thus, the parent wave is on the branch of a high-frequency part of electromagnetic whistler mode waves. The amplitude of the parent wave is $\delta B=0.31623B_0$, given an amplitude of the electron bulk velocity (velocity field) as $|\boldsymbol{U}_e|\sim0.2635c$. Therefore, we ignore the relativistic effect in Eq. (10) since the Lorentz factor is $\gamma\sim1$.

Figure 1 shows the temporal evolution of the magnetic field δB_z component at $y=0$ as a function of position x and time t. The parent wave (at Mode 32) propagates in the $+x$ direction at a phase velocity of $v_p/c\sim0.05$, which is in good agreement with the analytical phase velocity estimated from the dispersion relation in Eq. (10).[11] It should be noted that the parent wave is subjected to the linear cyclotron damping and quickly damps in a timescale of $1/\omega_0$ when the amplitude is much smaller than the ambient magnetic field ($\delta B_z\ll B_0$). On the other hand, the parent wave is not subjected to the cyclotron damping in the present case with a large amplitude, which suggests that the parent wave is on a branch of the "nonlinear" eigenmode. In contrast to our previous 1D simulation study where the backscattered daughter wave appears at $\omega_{pe}t\sim800$ (see Fig. 1 in Ref. 4), the parent wave suddenly decays at $\omega_{pe}t\sim70$ in the present 2D simulation.

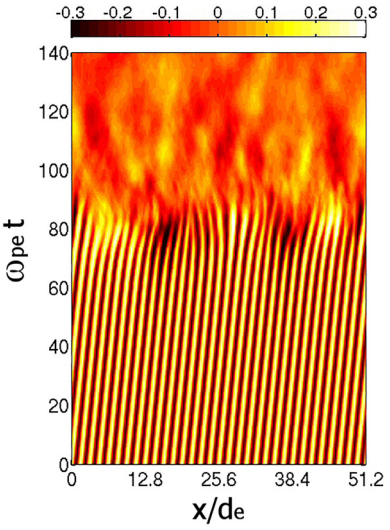

FIG. 1. Temporal evolution of the magnetic field δB_z component at $y=0$ as a function of position x and time t. The magnitude is normalized by B_0.

Figure 2 shows the energy history of the electromagnetic fields and particles. Panel (a) shows the energy densities of the magnetic field ($|\boldsymbol{B}|^2=B_x^2+\delta B_y^2+B_z^2$), the electric field ($|\boldsymbol{E}|^2=E_x^2+E_y^2+E_z^2$), and the electron drift energy density ($K_{e||}-P_{e||}$) in the direction parallel to the ambient magnetic field. Panel (b) shows the energy densities of the magnetic field B_x component and the electric field E_x and E_y components. Panel (c) shows the electron kinetic energy density and the electron pressure in the direction perpendicular to the ambient magnetic field ($K_{e\perp}$ and $P_{e\perp}=2N_eT_{e\perp}=N_e(T_{ey}+T_{ez})$). Panel (d) shows the temperature of electrons in the directions parallel and perpendicular to the ambient magnetic field ($T_{e||}$ and $T_{e\perp}$, respectively). Panel (e) shows the temperature of ions in the directions parallel and perpendicular to the ambient magnetic field ($T_{i||}$ and $T_{i\perp}$, respectively). The energy density and the temperature are normalized by $B_0^2/2\mu_0$ and T_0, respectively.

The total magnetic field energy decreases from $\omega_{pe}t\sim70$. The energies of the electric field E_x component, the magnetic field B_x component, and the parallel drift energy of electrons increase slightly earlier than the magnetic field energy decreases ($\omega_{pe}t\sim60$), while the increase in the ion kinetic energy in the present 2D simulation is much smaller than in the previous 1D simulation.[4] The result suggests the excitation of sound waves propagating in the

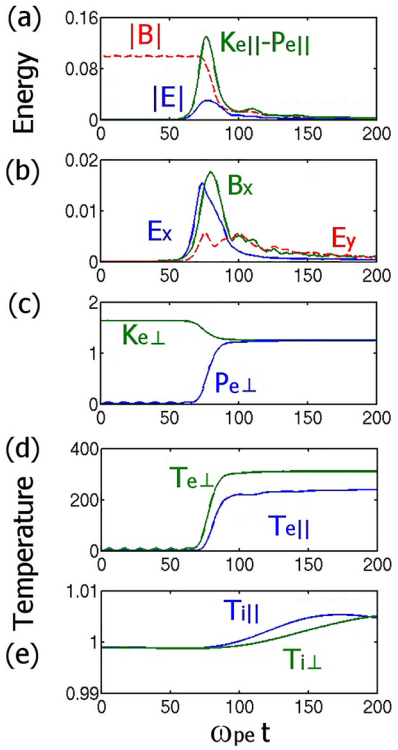

FIG. 2. Energy history of the electromagnetic fields and particles. (a) The energy densities of the magnetic field ($|\boldsymbol{B}|^2 = B_x^2 + \delta B_y^2 + B_z^2$), the electric field ($|\boldsymbol{E}|^2 = E_x^2 + E_y^2 + E_z^2$), and the electron drift energy density ($K_{e||} - P_{e||}$) in the direction parallel to the ambient magnetic field. (b) The energy densities of the magnetic field B_x component and the electric field E_x and E_y components. (c) The electron kinetic energy density and the electron pressure in the direction perpendicular to the ambient magnetic field ($K_{e\perp}$ and $P_{e\perp} = 2N_eT_{e\perp} = N_e(T_{ey} + T_{ez})$). (d) The temperature of electrons in the direction parallel and perpendicular to the ambient magnetic field ($T_{e||}$ and $T_{e\perp}$, respectively). (e) The temperature of ions in the direction parallel and perpendicular to the ambient magnetic field ($T_{i||}$ and $T_{i\perp}$, respectively). The energy density and the temperature are normalized by $B_0^2/2\mu_0$ and T_0, respectively.

directions parallel and (quasi-)perpendicular to the ambient magnetic field, which is, however, different from ion acoustic waves seen in the 1D parametric decay. The thermal energy (pressure) of electrons in the direction perpendicular to the magnetic field and the energy of the electric field E_y component also increases as the magnetic field energy decreases. During the decay of the parent wave, most of the initial perpendicular electron bulk energy ($K_{e\perp} - P_{e\perp}$) due to the velocity field of the parent wave is converted to the perpendicular electron thermal energy, which is similar to the previous 1D simulation.[4] In contrast to the previous 1D simulation,[4] however, ion heating in both directions parallel and perpendicular to the ambient magnetic field is very weak in the present 2D simulation.

The top panels of Fig. 3 show the spatial profile of the magnetic field δB_z component together with the wavenumber spectrum at $\omega_{pe}t = 70$, when the electric field E_x component saturates. There are two sideband modes at (k_{x0}, $\pm k_{y1}$) (where $k_{y1}d_e = 1.47$), suggesting that the parent wave is weakly modulated at Mode 3 in the y direction by these sideband modes. It is also seen that there are two other wave modes at (0, $\pm k_{y1}$), which may propagate in the direction quasi-perpendicular to the ambient magnetic field. These quasi-

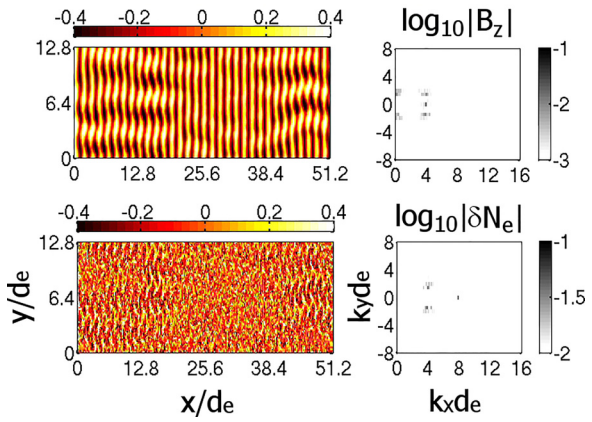

FIG. 3. Spatial profiles of the magnetic field δB_z component (top) and the electron density δN_e (bottom) at $\omega_{pe}t = 70$ together with the wavenumber spectra on a logarithmic scale. The magnitudes of the magnetic field and the density are normalized by B_0 and N_0, respectively.

perpendicular modes have a broadband spectrum in the k_x space (with a wavenumber range of $-0.614 < \Delta k_{x1}d_e < 0.614$).

The bottom panels of Fig. 3 show the spatial profile of the electron density δN_e at $\omega_{pe}t = 70$ together with the wavenumber spectrum. There are two sideband modes at (k_{x0}, $\pm k_{y1}$), which correspond to the electrostatic component of the daughter oblique whistler waves seen in the δB_z component. It is also found that a parallel electrostatic wave is strongly enhanced at ($2k_{x0}$, 0).

Since the timescale of the present decay instability is fast (at a timescale of $\sim 10/\omega_{pe}$), it is impossible to obtain the exact frequencies and propagation directions of the excited daughter waves by the Fourier analysis. The previous studies suggested the wave damping via the modulational instability where a parent wave with frequency ω_0 and wavenumber $\boldsymbol{k}_0$ decays into two daughter sideband waves with $(\omega_0 \pm \omega_{1S}, \boldsymbol{k}_0 \pm \boldsymbol{k}_{1S})$ and a daughter sound (longitudinal) wave with $(\omega_{1S}, \boldsymbol{k}_{1S})$.[12,13]

From the analytic linear dispersion relation in Eq. (10), the frequency of the two daughter sideband modes (oblique whistlers) in Fig. 3 is obtained as $\omega \sim 0.8359|\omega_{ce}|$ $(= 0.1869\omega_{pe})$, which gives the frequency difference of $\omega_1 \sim 0.0113\omega_{pe}$. It is suggested that the frequency difference is smaller than the ion plasma frequency. On the other hand, there is no enhancement in the ion density (while there exist thermal fluctuations on the order of magnitude of $\delta N_i/N_0 \sim 10^{-4}$). Hence, there arises a question about a contribution of ion dynamics in the present 2D decay process. We performed an additional simulation run with immobile ions ($m_i/m_e = \infty$ as a background component for neutralizing electric charge) to solve this question. The result is almost the same as the run with $m_i/m_e = 1836$, suggesting that the ion physics plays no role in the present 2D decay instability.

It is suggested that the present 2D decay instability is somewhat different from the 1D modulational instability in the previous studies, where the daughter sideband modes are excited at the frequencies $\omega_0 - \omega_1$ and $\omega_0 + \omega_1$.[12,13] In the present 2D simulation, both daughter sideband modes are excited at the frequency $\omega_0 - \omega_1$. As shown in Fig. 3,

there exist other quasi-perpendicular daughter waves at $(k_x, k_y) \sim (\Delta k_{x1}, k_{y1})$ and $(\Delta k_{x1}, -k_{y1})$ in the magnetic field B_z component. These modes also exist in the magnetic field B_x component. However, the structure (waveform) of the quasi-perpendicular daughter waves is almost steady (with a frequency close to zero), and the B_z and B_x components are dominant. It is suggested that the quasi-perpendicular daughter waves are on branches of the nonlinear eigenmode since a quasi-perpendicular electromagnetic wave mode with a frequency close to zero does not exist in the linear dispersion relation without ions.

There is also enhancement of the longitudinal electric field (E_x) component at $(k_x, k_y) = (2k_{x0}, 0)$. From the waveform of the complex Fourier amplitude $E_x(t, 2k_{x0}, 0)$, we estimate the frequency of this mode as $\omega \sim 0.4\omega_{pe}$. This frequency is close to $2\omega_0$, suggesting that this mode is also on a branch of the nonlinear eigenmode. It is also suggested that the enhancement of this mode is not directly by the present 2D decay instability but by its secondary process, i.e., the three-wave interaction with $(\omega_0, k_{x0} \pm \Delta k_{x1}, k_{y1})$ and $(\omega_0, k_{x0} \mp \Delta k_{x1}, -k_{y1})$. To confirm this three-wave interaction, we have performed additional simulation runs with different plasma beta ($\beta_{e0} = 0.001$ and 0.016). The results show that the longitudinal electrostatic wave is enhanced at $(k_x, k_y) = (2k_{x0}, 0)$ with a frequency $2\omega_0$ in both runs.

In summary, a large-amplitude, monochromatic, and parallel parent whistler wave with $(\omega_0, k_{x0}, 0)$ decays into two sideband daughter quasi-parallel whistlers with $(\omega_0 - \omega_1, k_{x0} - \Delta k_{x1}, \pm k_{y1})$ and two quasi-perpendicular modes with $(\omega_1, \Delta k_{x1}, \pm k_{y1})$ via a 2D decay instability. It is noted that the present five-wave coupling process is also regarded as double three-wave couplings, i.e., $(\omega_0, k_{x0}, 0) \rightarrow (\omega_0 - \omega_1, k_{x0} - \Delta k_{x1}, k_{y1}) + (\omega_1, \Delta k_{x1}, -k_{y1})$ and $(\omega_0 - \omega_1, k_{x0} - \Delta k_{x1}, -k_{y1}) + (\omega_1, \Delta k_{x1}, k_{y1})$. A longitudinal electrostatic wave is also enhanced at $(2\omega_0, 2k_{x0}, 0)$ by a secondary three-wave interaction with the sideband daughter quasi-parallel whistlers. The low-frequency quasi-perpendicular mode and the longitudinal electrostatic mode are on branches of the nonlinear eigenmode, which disappear when the decay process of the parent wave is completed. The timescale of the present 2D decay instability is shorter than a hundred of the electron plasma period, which is much faster than the 1D parametric decay whose timescale is several hundreds of the electron cyclotron period.

It should be noted that the excitation of the quasi-perpendicular mode is similar to the filamentation instability of the dispersive circularly polarized Alfvén waves[14] since there exist current filaments along the ambient magnetic field as indicated in the B_z comportment (Fig. 3). However, the filamentation instability includes the coupling with the ion density fluctuations (i.e., linear eigenmode), which is different from the 2D decay instability seen in the present study. In the light of the independence on the electron beta, a multi-dimensional decay instability in the electron magneto-hydrodynamic (EMHD) system[15] is one of the candidates for the wave-wave coupling observed in the present study, although the strong enhancement of the parallel electric field energy may not be valid in the EMHD system. In addition, the initial bulk velocity of electrons is weakly relativistic in the present study. A transverse instability can be driven by a strong anisotropy in the initial kinetic energy of electrons[16] via a similar mechanism to the beam-Weibel instability,[17] which is another candidate.

This work was supported by MEXT/JSPS under Grant-In-Aid (KAKENHI) Nos. 26287041, 26287119, and 15K13572. The computer simulation was performed on the CIDAS system at the Institute for Space-Earth Environmental Research in Nagoya University through the joint research program.

[1]T. Terasawa, M. Hoshino, J.-I. Sakai, and T. Hada, J. Geophys. Res. **91**, 4171, doi:10.1029/JA091iA04p04171 (1986).
[2]H. K. Wong and M. L. Goldstein, J. Geophys. Res. **91**, 5617, doi:10.1029/JA091iA05p05617 (1986).
[3]D. W. Forslund, J. M. Kindel, and E. L. Lindman, Phys. Rev. Lett. **29**, 249 (1972).
[4]T. Umeda, S. Saito, and Y. Nariyuki, Astrophys. J. **794**, 63 (2014).
[5]H. Usui, H. Matsumoto, and R. Gendrin, Nonlinear Process. Geophys. **9**, 1 (2002).
[6]I. H. Cairns, P. A. Robinson, and N. I. Smith, J. Geophys. Res. **103**, 287, doi:10.1029/97JA02871 (1998).
[7]T. Umeda and T. Ito, Phys. Plasmas **15**, 084503 (2008).
[8]S. Saito, Y. Nariyuki, and T. Umeda, Phys. Plasmas **22**, 072105 (2015).
[9]I. V. Sokolov, Comput. Phys. Commun. **184**, 320 (2013).
[10]T. Umeda, Y. Omura, T. Tominaga, and H. Matsumoto, Comput. Phys. Commun. **156**, 73 (2003).
[11]S. Saito, S. P. Gary, and Y. Narita, Phys. Plasmas **17**, 122316 (2010).
[12]J.-I. Sakai and B. U. O. Sonnerup, J. Geophys. Res. **88**, 9069, doi:10.1029/JA088iA11p09069 (1983).
[13]M. Longtin and B. Sonnerup, J. Geophys. Res. **91**, 6816, doi:10.1029/JA091iA06p06816 (1986).
[14]A. F. Vinas and M. Goldstein, J. Plasma Phys. **46**, 129 (1991).
[15]J. S. Zhao, J. Y. Lu, and D. J.Wu, Astrophys. J. **714**, 138 (2010).
[16]B. D. Fried, Phys. Fluids **2**, 337 (1959).
[17]C. T. Huynh and C. M. Ryu, Phys. Plasmas **21**, 092115 (2014).